Multimode polymer bent tapered waveguide modeling

Ioannis Papakonstantinou, David R. Selviah and F. Anibal Fernandez
Department of Electronic and Electrical Engineering, University College London,
Torrington Place, London WC1E 7JE, United Kingdom
i.papakonstantinou@ee.ucl.ac.uk, d.selviah@ee.ucl.ac.uk, a.fernandez@ee.ucl.ac.uk.

Abstract *FD-BPM modeling of multimode polymer bent tapered waveguides gives lower insertion loss, reduced tolerance to lateral misalignment of the optical source but a better angular tolerance than straight tapers with the same input/output aperture ratio.*

Introduction

Large electronic systems often consist of racks of printed circuit board (PCB) daughter cards plugged into an interconnecting backplane motherboard PCB. Above 10 Gb/s passive polymer optical waveguide backplanes offer a promising alternative to multilayer copper track PCB backplanes which suffer from high loss and electromagnetic interference [1]. Lasers and photodiodes, mounted on the daughter cards, may be slightly misaligned to the backplane waveguides when the daughter cards are inserted giving variable connector loss. Lenses may be used but to minimize the component count tapered waveguides are proposed since their wide input aperture gives a good tolerance to lateral translational misalignment [2] while their narrow output aperture matches the small active area of high-speed photodetectors. However, when daughter boards having connectors located in the same position on each of them, are closely spaced it is necessary to bend the waveguide immediately after the taper to avoid the next connector. The closest spacing is achieved by combining both functions into a single component – the bent taper. This paper investigates whether the lateral misalignment tolerance is maintained in the bent taper and also investigates angular misalignment and insertion loss for a range of taper aperture ratios using finite difference beam propagation (FD-BPM) modeling.

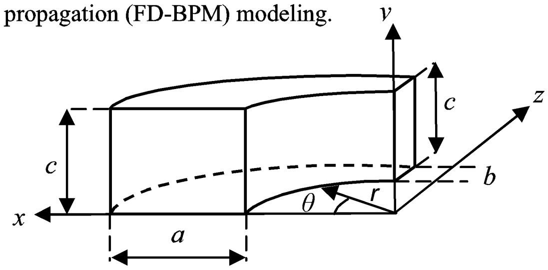

Fig. 1 Bent tapered waveguide

Theoretical Background

A waveguide which bends and tapers in the azimuth is presented in Fig. 1. The width of the waveguide tapers linearly with θ from a down to width b, with constant thickness, c. The input aperture is 50 μm × 50 μm and various taper aperture ratios, a/b were modeled. The refractive index of the core was chosen to be 1.54 and that of the cladding 1.9% less giving a N.A. of 0.3, typical of polymer waveguides. These refractive indices give weak coupling between the polarizations so the scalar approximation is justified. Optical field solutions, $G(r,\theta,y)$ obey the cylindrical scalar wave equation:

$$\left[\frac{1}{r}\frac{\partial}{\partial r}\left(r\frac{\partial}{\partial r}\right)+\frac{\partial^2}{\partial y^2}-\frac{\beta^2R^2}{r^2}+k_o^2n^2(r,y)\right]G(r,y)=0 \qquad (1)$$

neglecting time dependence. Waveguiding along the curved central axis requires a θ dependence of the form: $G(r,\theta,y) = G(r,y)e^{-i\beta R\theta}$ where R is the radius of curvature of the central curved axis shown in Fig. 2.

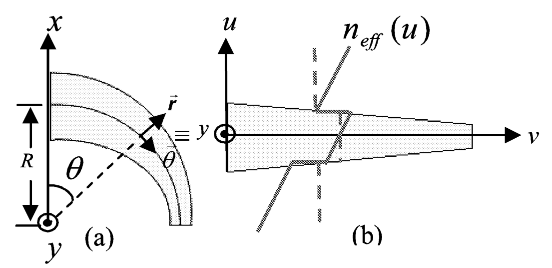

Fig. 2 Bent tapered waveguide (a) and its transformation to the new coordinates (b). Solid line shows the local effective refractive index.

The cylindrical wave equation is solved by applying a special form of the separation of variables technique [3]: $G(r,y) = r^{-1/2}G_1(r)G_2(y)$ to give

$$\left[\frac{d^2}{dr^2}+\left(k_o^2n_{eff}^2(r)-\beta^2\right)\right]G_1(r)=0 \qquad (2)$$

where the local effective refractive index is:

$$n_{eff}^2(r)=n^2(r)+\left[\frac{\beta^2}{k_o^2}\left(1-\frac{R^2}{r^2}\right)+\frac{1}{4k_o^2r^2}\right]+\frac{\beta_y^2}{k_o^2} \qquad (3)$$

The conformal transformation, $u = r - R$ and $v = R\theta$ maps the bent taper to an equivalent linear taper in the (u,v) coordinate system [3] but having a local effective refractive index variation shown by the solid line rather than the dashed line in Fig. 2(b).

Simulation method

The structure in Fig. 2(b) was analyzed with wide-angle FD-BPM. The coordinate transformation has two effects. Firstly it alters the paraxial limits for BPM since the propagation axis z is not curved and secondly the simulation domain is considerably reduced because the area covered by a straight waveguide is much less than the area covered by a bend. Higher order (1,1) Padé coefficients were used neglecting reflections. The transverse grid elements were 100 nm x 100 nm and the axial step size was chosen to be 1 µm. A 7 µm FWHM Gaussian beam at λ = 850 nm, representing the fundamental transverse mode of a VCSEL, was used as the launching field. The propagation axis radius was chosen to be R = 20 mm since larger radii gave similar results. A straight section of 5 mm was attached to the end of the structure to take account of transition losses at the junction with a straight waveguide. Material intrinsic loss was neglected to reveal the excess losses occurring due to bending and tapering and roughness of the waveguide wall was also neglected. The optical input field was translated laterally along x from the centre of the input face and the phase front angled to investigate lateral and angular misalignments.

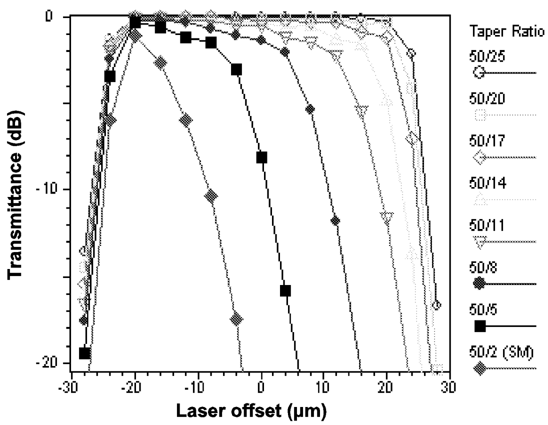

Fig. 3 Bent taper transmittance as a function of laser offset for various taper ratios, *a/b*

Results and Conclusions

Fig. 3 shows the transmittance as a function of the lateral misalignment of the field. The input/output taper ratio, *a/b* was varied from 50/25 to an extreme of 50/2 corresponding to tapering down to a single lateral mode waveguide for our choice of indices. The maximum transmittance is achieved when the laser source is displaced by 20 µm from the centre of the input guide towards the outer edge of the bend. As the taper ratio increases the device becomes less and less tolerant to misalignments about this optimum point. The asymmetric behavior is due to the asymmetric distribution of the local modes in the bent waveguide. Fig. 4 compares the lateral misalignment tolerance as a function of taper ratio, *a/b* for a bent taper and a linear taper for the same launch conditions. The lateral misalignment tolerance is defined as the Full Width Half Maximum (*FWHM*) of the transmittance curves shown in Fig. 3. Fig. 4 also compares the maximum power transmitted through the bent and straight tapers. As the taper ratio increases the lateral misalignment tolerance drops for both bent and straight tapers. The linear taper shows a better lateral misalignment tolerance but at the expense of a somewhat higher insertion loss. Fig. 5 shows the angular tolerance which is the FWHM of the transmittance for angular misalignments of the input field as a function of the taper ratio. For the bent taper the source was offset by -20 µm to the optimum point before rotation. For the straight taper the source was at the centre of the input face. The bent taper can tolerate more angular misalignment than the straight taper. So comparing bent with straight tapers for a given taper ratio there is a trade off between angular and lateral translational misalignment tolerances and also a trade off between lateral translational misalignment and insertion loss. All degrade with increasing taper ratio.

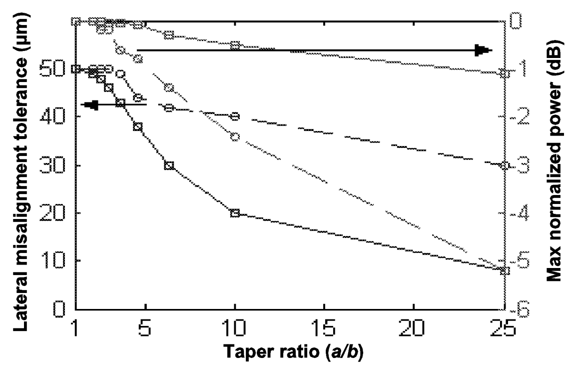

Fig. 4 Lateral misalignment tolerance and transmittance when centrally aligned for bent tapers (solid line) and linear tapers (dashed line).

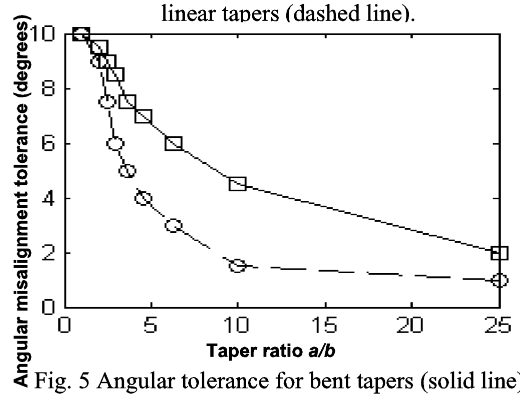

Fig. 5 Angular tolerance for bent tapers (solid line) and linear tapers (dashed line).

Acknowledgement

The authors thank Xyratex Technology Ltd and EPSRC/DTI via the LINK Storlite project for financial support.

References

1 G. Panotopoulos, *IEEE LEOS 15th Annual Workshop on Interconnections Within High Speed Digital Systems, Workshop Notes,* MA1, Santa Fe, 2004.

2 Atef M. Rashed and David R. Selviah, *Abstracts SIOE '04*, paper 40, Cardiff, Wales, 2004.

3 K. Thyagarajan, M. R. Shenoy and A. K. Ghatak, *Optics Letters*, Vol. 12, No. 4, pp. 296-298, 1987.